Springer

Journal of
Mechanical
Science and
Technology

Journal of Mechanical Science and Technology 22 (2008) 887~894

www.springerlink.com/content/1738-494x

Manipulability analysis of underwater robotic arms on ROV and application to task-oriented joint configuration

Bong-Huan Jun[1], Pan-Mook Lee[1] and Seungmin Kim[2,*]

[1]*Maritime and Ocean Engineering Research Institute, KORDI, 171, Jang-dong, Yuseong, Daejeon, 305-343, Republic of Korea*
[2]*Dept. of Mechatronics Exam., The Korean Intellectual Property Office, #920, Dunsan-dong, Seo-gu, Daejeon, 302-701, Republic of Korea*

(Manuscript Received April 6, 2007; Revised December 5, 2007; Accepted February 2, 2008)

Abstract

This paper describes the task-oriented manipulability of tele-operated robotic arms mounted on a remotely operated vehicle (ROV) and its application to task-oriented joint configurations. The main purpose of the study is to reduce the tele-operator's burden in performing underwater tasks by enhancing the functionality of the manipulator. Even though a manipulator has 6 degrees-of-freedom (DOF), which is proper DOF to work in Cartesian workspace, the manipulator might have redundancy according to task types and order of task-priority. This paper focuses on the problem to utilize the redundancy by introducing a scalar function as an object of optimization. The scalar function is composed of a task-oriented manipulability measure (TOMM) and joint limit measure (JLM). Using sequential quadratic programming (SQP) with the object function, we obtained optimal postures of the manipulator for a given position constraint of the end-effecter. Adopting the scalar function as a performance index, we solved a redundancy resolution problem based on the pseudo inverse of the task-oriented Jacobian matrix.

Keywords: Rbotics arm; ROV; Manipulators; Joint limit measure

1. Introduction

Underwater vehicles with manipulators have become an important tool for performing a variety of underwater tasks in the fields of scientific research and ocean engineering. Most of the work-class and scientific remotely operated vehicles (ROVs) are equipped with one or two tele-operated manipulators to perform their unstructured underwater missions, such as drilling, cutting in the case of work ROVs and sampling, coring, connector-mating in scientific ROVs. Although there are many works to enhance the autonomy of an underwater manipulator system, called an underwater vehicle-manipulator system (UVMS) as in [1-4], the tele-operated manipulator system is still the workhorse in underwater work since most underwater tasks are highly complex and unstructured. A tele-operated manipulator system is composed of two arms having the same kinematic structure: a passive master-arm and an underwater slave-arm. Since the tele-operator has to control all the slave joints with the master-arm on the surface based on video images fed back from the slave arm site, it is not easy to control the tele-operated manipulator system even with a skilled operator. To complete the given mission successfully, the operator has to control all the joints considering the joint limitation and relative position and orientation of the end-effecter. When the task requires more precise position and orientation of the end-effecter, the operator's burden is dramatically increased.

This paper considers the problem of increasing the working efficiency of tele-operated underwater manipulation by assisting the human operator to reduce the burden in controlling the manipulator precisely and

*Corresponding author. Tel.: +82 42 481 8442, Fax.: +82 42 472 352
E-mail address: kipo0070@kipo.go.kr
DOI 10.1007/s12206-008-0201-7

efficiently. Even though the manipulator has 6 degrees-of-freedom (DOF) or less, the manipulator can have redundancy according to the type or priority of task to be performed. If there is a task that requires precise position but not orientation of the end-effecter, then the manipulator with 6-DOF has redundancy of 3-DOF. The problem utilizing these kinds of redundancies is called task-priority redundancy resolution [5, 6]. In order to utilize the redundancy to enhance the functionality or to avoid joint limit of a tele-operated manipulator, a scalar function composed of task-oriented manipulability measure (TOMM) and joint limit measure (JLM) is introduced. It is assumed that a new master system composed of a computer and an input device for velocity workspace command is installed in the given tele-operated manipulator system for realization.

Two approaches are presented to enhance the functionality of the tele-operated underwater manipulator using the presented scalar function; one is off-line optimization to find optimal configurations of the manipulator under given constraints, and the other is an on-line control problem utilizing redundancy resolution. Sequential quadratic programming (SQP) is used for off-line optimization. Since the SQP algorithm solves local minimization problems, the optimizations are performed with various optimal candidates of initial configurations to find the optimal configuration. The obtained optimal configuration can be used as an initial deploy point of manipulators to start a given work. In order to utilize the redundancy for real time control, we use the task-oriented redundancy resolution method based on the pseudo inverse of the task-oriented Jacobian matrix adopting the proposed scalar function as a performance index. Numerical simulation with the manipulator of KORDI ROV is carried out to investigate the effectiveness of the presented method.

2. Task-oriented manipulability analysis

2.1 Velocity and force manipulability

Assuming that a tele-operated *n*-DOF arm is working in an *m*-dimensional task space, we can generally express the relationship between joint variable vector $q \in R^n$ and manipulation variable vector $r \in R^m$ by

$$r = f(q) . \tag{1}$$

Differentiating (1) with respect to time, we represent the relationship between the end-effecter velocity $\dot{r}$ and joint velocity $\dot{q}$ by linear algebraic equation as

$$\dot{r} = J(q)\dot{q} \tag{2}$$

where $J(q)$ is Jacobian matrix defined as $\partial f / \partial q \in R^{m \times n}$. Yoshikawa defined the manipulability measure (MM) and ellipsoid (ME) using manipulator Jacobian in [7] and [8]. Lee defined the task-oriented manipulability measure as a geometrical closeness between the desired and the actual manipulability ellipsoids [9]. When the *n*-DOF tele-operated manipulator is working with *k*-subtasks, we can rewrite (2) as

$$\dot{r}_i = J_i(q)\dot{q} \qquad i = 1,2,...,k , \tag{3}$$

where $k \le n$ is the number of subtasks. In this paper, MM and ME corresponding to each subtask are defined as task-oriented manipulability measure (TOMM) and task-oriented manipulability ellipsoid (TOME) of the tele-operated manipulator system. TOMM and TOME are represented as the same manner in [5] and [7] by

$$\text{TOMM:} \quad w_i = \sqrt{\det(J_i J_i^T)} \tag{4}$$

$$\text{TOME:} \quad \dot{r}_i^T (J_i J_i^T)^{-1} \dot{r}_i \le 1 \qquad i = 1,2,...,k , \tag{5}$$

where J_i^T is the transpose of J_i. TOMM is proportional to the volume of TOME mathematically defined as a mapping of the unit sphere of joint velocity to an ellipsoid in the Cartesian velocity space by task-oriented Jacobian transformation J_i. TOMM denotes the ability of motion in terms of specific subtask, while MM denotes the ability of motion of the whole manipulator system. Therefore, TOMM can be used as a potential function to enhance the manipulator functionality in terms of a subtask.

From the analogy with differential kinematic relationship, the relationship between the joint torque vector τ and the Cartesian static force vector F_i can be described as

$$\tau = J_i^T F_i \qquad i = 1,2,...,k . \tag{6}$$

Then the task-oriented force manipulability measure (TOFMM) and ellipsoid (TOFME) are derived as (7) and (8), respectively.

$$\text{TOFMM:} \quad w_{f,i} = \sqrt{\det((J_i J_i^T)^{-1})} \tag{7}$$

$$\text{TOFME:} \quad F_i^T (J_i J_i^T) F_i \le 1 \tag{8}$$

TOFMM denotes the quantitative measure of manipulator functionality in terms of task force under the joint torque constraint given in 2-norm sense.

As an example, consider a task requiring the end-effecter to preserve the position and orientation in x-axis of base coordinates. The task-oriented Jacobian can be written by

$$J_1 = \begin{bmatrix} J(1) \\ J(5) \end{bmatrix}, \tag{9}$$

where $J(1)$ and $J(5)$ are the first and the fifth row vectors of the Jacobian matrix, respectively. Substituting (9) to (4), (5) and (6), (7), we can obtain TOMM, TOME, TFMM and TFME, respectively, in terms of a given task.

2.2 Task-oriented manipulability analysis of an arm

In this section, the kinematic structure and manipulability of an arm of KORDI ROV are described. KORDI ROV, a scientific vehicle under development in KORDI, will be equipped with dual ORION manipulator made by ALSTOM Schilling Robotics. Fig. 1 shows the conceptual view of KORDI ROV and Fig. 2 describes configuration and basic dimensions of the ORION manipulator. The arm, of which Denavit-Hartenberg parameters are listed in Table1, has six functional joints and one gripper.

If the joint configuration and the task are given, TOMM and TOME can be obtained by (4) and (5), respectively. Selecting the task as translational motion of the end-effecter, we obtained the 3- dimen-sional TOME shown in Fig. 3(a) with an example

Fig. 1. Conceptual view of KORDI ROV with a dual tele-operated manipulator.

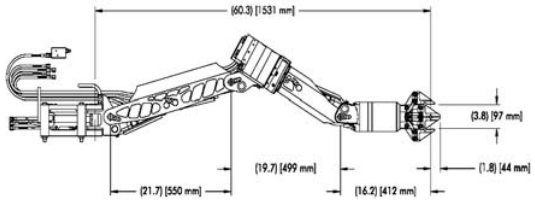

Fig. 2. Basic configuration and dimension of slave manipulator, ORION Schilling Robotics [11].

Table 1. Denavit-Hartenberg parameters.

Joint	θ_i	q_i (deg)	a_i (mm)	d_i (mm)	Joint limit
1	θ_1	90	71.1	0	-60, +60
2	θ_2	0	566.4	0	-30, +90
3	θ_3 +90	90	134.6	0	-90, +30
4	θ_4	-90	0	500.4	-135, +135
5	θ_5	90	0	0	-30, +90
6	θ_6	0	0	408.9	-180, +180

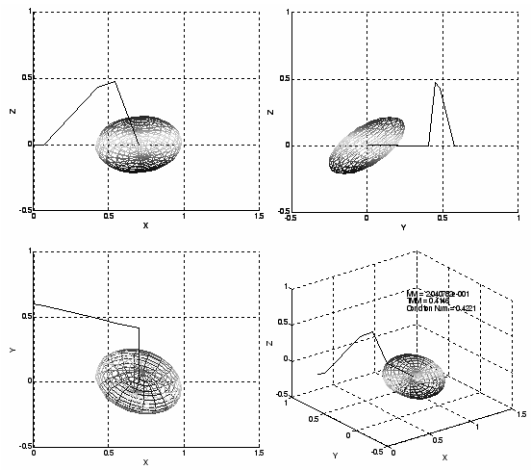

(a) TOME (translational manipulability ellipsoid)

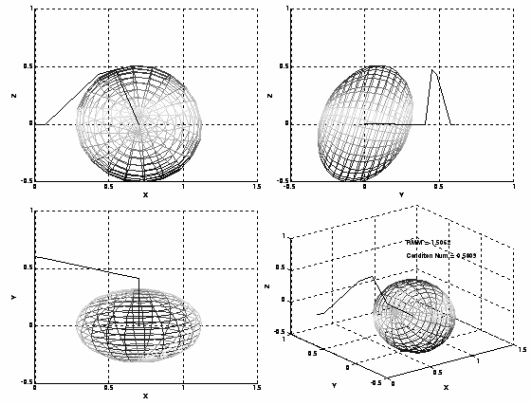

(b) TOME (orientational manipulability ellipsoid)

Fig. 3. Task-Oriented Manipulability Ellipsoid for an example posture [-15.3, 49.6, -31.0, 75.5, 85.2, –18.0] (MM = 2.04, TMM = 0.41, RMM = 1.51).

posture of [-15.3 49.6 -31.0 75.5 85.2 –18.0] in degrees. The TOMM is 0.41 while MM is 2.04. The major axis of the translational ellipsoid indicates the direction that maximum translational motion can be obtained by the end-effecter. When orientational motion is selected as the task, TOME is obtained as Fig. 3(b). As a matter of course, the major axis of ellipsoid indicates the direction that maximum orientational motion can be exerted while the minor axis denotes the direction of minimum orientational motion. In the same manner, TOFME and TOFMM can be obtained by (7) and (8), but the length of the principal axis is reciprocal.

3. Task-oriented optimal posture

3.1 Constrained optimization problem

The previous chapter considered the problem of finding the manipulability ellipsoid and measure of manipulators in a given posture. At the practical application of manipulator, however, it would be more useful to find the optimal posture of manipulators to obtain maximum manipulability in given constraints such as the joint limit and given task of the end-effecter. This kind of problem is a general constrained optimization described as follows:

Find an optimal posture q, which minimizes the function $f(q)$ subject to:

$$\begin{aligned} &g_i(q)=0, \quad i=1,2,....,m \\ &g_j(q)\le 0, \quad j=1,2,....,n \\ &q_l \le q \le q_u \end{aligned} \tag{10}$$

where q is an n-dimensional joint angle vector of unknowns, $q=(q_1,q_2,...,q_n)$, and f, g_i, g_j are real-valued functions of the variable q. The vectors q_l and q_u are the lower and upper bounds of q, respectively. The function f is the objective of the problem, and the equalities and inequalities are constraints.

3.2 Joint limit

In order to obtain a feasible optimal solution in real situation, the mechanical joint limit has to be considered. Even though each joint limit is different from each other, a joint limit vector can be transformed so that the transformed variable may be described in a unitary way. If the joint limit is given by

$$q_{i,\min} \le q_i \le q_{i,\max}, \qquad i=1,2,...,n, \tag{11}$$

we transform the joint variables into the new variables through

$$x_i \equiv D_i q_i + x_i^0, \tag{12}$$

where

$$D_i \equiv diag\left[\frac{2}{q_{1,\max}-q_{1,\min}} \cdots \frac{2}{q_{n,\max}-q_{n,\min}}\right] \tag{13}$$

$$x_i^0 \equiv \left[-\frac{q_{1,\max}+q_{1,\min}}{q_{1,\max}-q_{1,\min}} \cdots -\frac{q_{n,\max}+q_{n,\min}}{q_{n,\max}-q_{n,\min}}\right]^T. \tag{14}$$

In (13), $diag(\cdot)$ denotes a diagonal matrix with the specified diagonal elements. Then we obtain

$$-1 \le x_i \le 1 \qquad i=1,2...,n. \tag{15}$$

Now, we propose the following potential function as a joint limit measure (JLM):

$$p_{\text{joint}} = \prod_{i=1}^{n}(1-x_i^2) \tag{16}$$

The scalar function p_{joint} goes to zero when one of the joints approaches to its limit.

3.3 Optimal posture in the sense of TOMM and JLM

When operators work with manipulators on ROV, they fix the vehicle first on the sea bottom and then deploy the manipulator to a pre-determined posture before starting to control each joint of the master arm. It would be more helpful to the operator that the deploy point is as far as possible from singular point and joint limit of the manipulator. In this section, the optimal manipulator posture is obtained with the constrained optimization described in the previous section. We design the objective function $f(q)$ composed of TOMM and JLM as

$$f(q) = -\alpha p_{TOMM} - (1-\alpha) p_{\text{joint}}, \tag{17}$$

where p_{TOMM} is potential function due to the task-oriented manipulability defined in (4), and p_{joint} is potential function due to the joint limit measure defined in (16). The α in (17) is a weight factor to distribute the significance of TOMM and JLM.

Since the operator of ROV controls the manipulator based on camera vision, the best viewing position of the end-effecter can be a constraint of the optimization

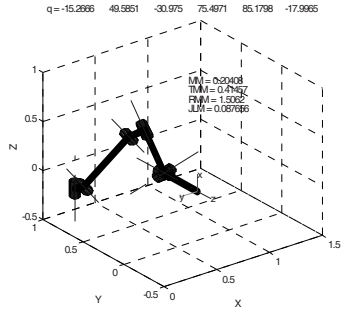

(a) Arbitrary posture

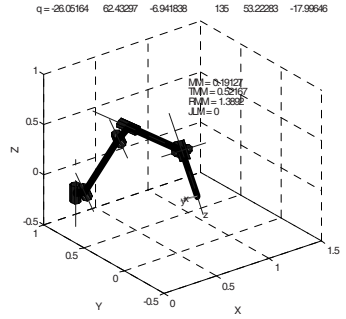

(b) Optimal posture with $\alpha = 1$

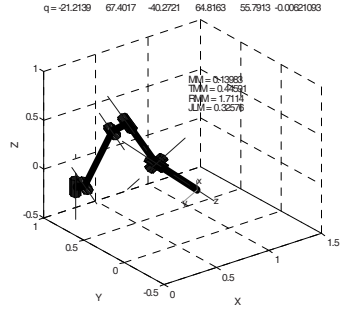

(c) Optimal posture with $\alpha = 0$

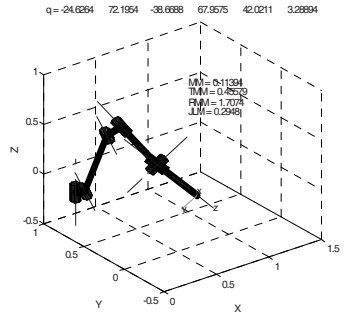

(d) Optimal posture $\alpha = 0.8$

Fig. 4. Optimal posture of ORION manipulator (TOMM : (a) 0.41, (b) 0.52, (c) 0.45, (d) 0.46, JLM : (a) 0.09, (b) 0, (c) 0.33, (d) :0.30).

problem. We consider the position of the end-effecter as an equality constraint described by

$$r_p - r_p^0 = 0, \tag{18}$$

where $r_p \in R^3$ and $r_p^0 \in R^3$, functions of q, are current and the target position vector of the end-effecter with respect to base coordinates. Note that (18) does not consider the orientation but only the position of the end-effecter. In this case, the 6-DOF manipulator system can utilize the 3-DOF to optimize its posture. To obtain the optimal posture with objective function (16) under the constraint of (18), the SQP algorithm is used under the boundary determined by joint limit by (11).

Since the SQP solves the local minimum solution, several initial candidates of optimal posture are used in the process. The optimization results with joint limit listed in Table 1 are shown in Fig. 4. The translational Jacobian is used for TOMM of objective function (16). Fig. 4(a) denotes the example posture of the ORION manipulator in Fig. 3. Fig. 4(b) shows the results in the case of $\alpha = 1$, which means only TOMM is considered as objective function. It is observed that the posture has the highest TMM (translational manipulability measure), but JLM is zero, which means at least one of the joints reached at its limit angle. When $\alpha = 0$, which means only the joint limit is considered as the objective function, the posture has the highest JLM with the concession of TMM (Fig. 4(c)). Selecting $\alpha = 0.8$, we can distribute the significance of TMM and JLM as Fig. 4(d). If the optimal posture (d) is adopted as deploy point and manipulation is started at the point, it is more convenient to change the posture to any arbitrary position. Moreover, if the task needs lower DOF or the manipulator has higher DOF, the operator can start manual control with higher TOMM and JLM.

4. Task-oriented control

4.1 Task description

The required task with manipulators can be divided into subtasks. One of the examples is to classify the task into the following two categories: position-oriented task and orientation-oriented task. For the case of thermal bent exploration, the former would be temperature measuring at a point, while the latter would be the direction of a camera-in-hand to objects. Both of the tasks can be also divided into other subtasks. For example, the position-oriented task can

be divided into a horizontal position-oriented task required to keep x, y position and vertical position-oriented task required to keep z position. According to the type of task, the order of redundancy would be changed. The redundancy can be used to optimize the configuration or perform other tasks according to order of priority, which is a problem of task priority control [5, 6]. In this chapter, the redundancy is utilized only for a given subtask adopting TOMM as a performance index to solve the redundancy resolution problem – task-oriented redundancy resolution.

4.2 Task-oriented redundancy resolution

If the $\dot{r}_1 \in R^k$ is manipulation variable to be performed with a manipulator, we can write the differential relationship between joint variables and manipulation variables as

$$\begin{bmatrix} \dot{r}_1 \\ \dot{r}_2 \end{bmatrix} = \begin{bmatrix} J_1 \\ J_2 \end{bmatrix} \dot{q}, \tag{19}$$

where $J_1 \in R^{k \times n}$ and $J_2 \in R^{(m-k) \times n}$ denote the Jacobians of manipulation variables and the other workspace variables, respectively. The general solution for manipulation is obtained as follows:

$$\dot{q} = J_1^+ \dot{r}_1 + \left\{ E_n - J_1^+ J_1 \right\} y, \tag{20}$$

where $E_n \in R^{n \times n}$ is identity matrix and y is an arbitrary vector. The second term of the right side of (20) represents the redundancy left after performing a given task. If there is a second task which needs to be also performed, the problem is general task-priority control, and the least-square solution of y is obtained by substituting (20) to $\dot{r}_2 = J_2 \dot{q}$ in (19).

If only the first task is important, the redundancy can be used only for the first task to be performed with more kinematic ability – *task-oriented control*. This problem can be realized by the redundancy resolution method in [5] by adopting the performance index as (16). Note that J_2 is excluded from the performance index. The task-oriented solution is obtained by determining the arbitrary vector y in (20) using the potential approach as

$$\dot{q} = J_1^+ \dot{r}_1 + \left\{ E_n - J_1^+ J_1 \right\} \left(-\varepsilon \frac{\partial p}{\partial q} \right)^T, \tag{21}$$

where ε is a positive scalar.

A numerical simulation was carried out with the ORION manipulator, It was assumed that the operator needs to move the end-effecter in Cartesian space with velocity of [0.1, 0.08, -0.08]. Note that the task needs only translational motion of the end-effecter without orientational motion. Then the task-oriented Jacobian J_1 is composed of three upper row vectors of the manipulator Jacobian. The initial configuration of the manipulator is the optimal posture in the sense of joint limit, which is shown in Fig. 4(c). The calculation was performed until 5 seconds with 0.05 seconds of sampling period. The results are shown in Figs. 5-7. Fig. 5 shows the series of postures solved by the pseudo inverse of the entire Jacobian matrix J with $\dot{r} = [0.1, 0.08, -0.08, 0, 0, 0]$, while Fig. 6 shows the solution posture by (21) with $\alpha = 0.5$. The solution posture obtained with the pseudo inverse of J_1 neglecting second term of (21) is omitted because it shows slightly different from the configuration of Fig. 6. However, the

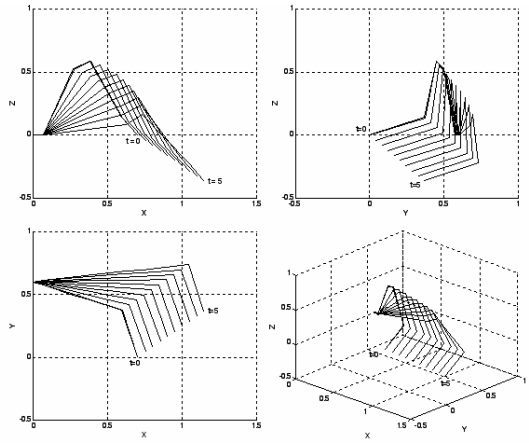

Fig. 5. Solution of J^+

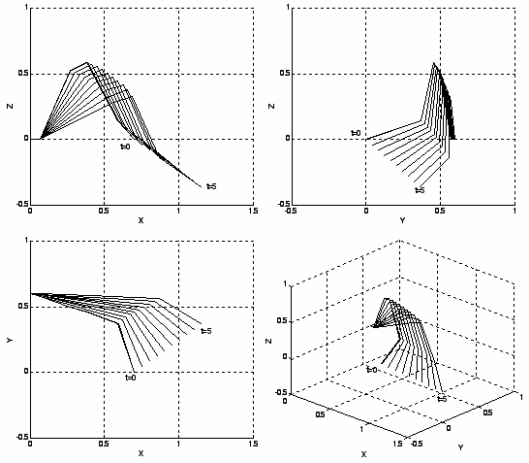

Fig. 6. Solution of Eq. (21).

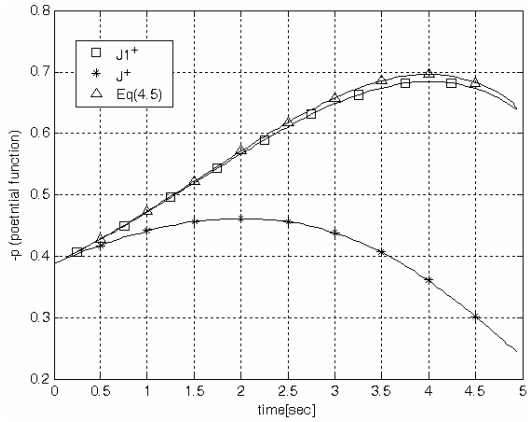

Fig. 7. Trajectory of performance index.

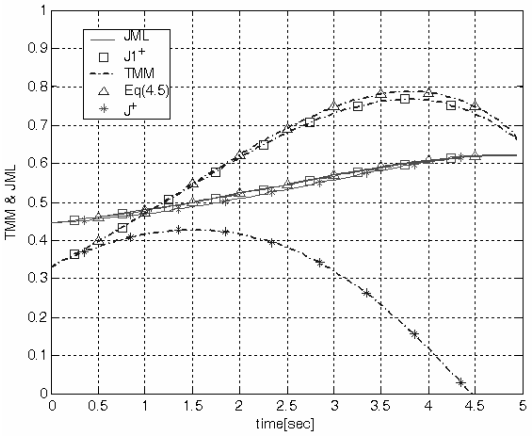

Fig. 8. Trajectory of Translational MM and JLM.

performance index of the case is compared in Fig. 7, and TOMM and JLM in Fig. 8. From the performance index depicted in Fig. 7, we can expect the solution of (21) has the highest ability of motion and is farthest from the joint limit, which is verified by the trajectories of TMM and JLM shown in Fig. 8. Noting that the JLM of J^+ solution go to zero at 4.5 seconds, we can recognize that one of the joints is reached at its joint limit and final posture of Fig. 5 cannot be realized in a real situation.

4.3 Application to ORION manipulator

The ORION manipulator system on KRODI ROV commands each joint angle of the slave manipulator with the master manipulator in joint space. Supposing a new master system is installed composed of a computer and an input device able to command end-effecter velocity in workspace as depicted in Fig. 9,

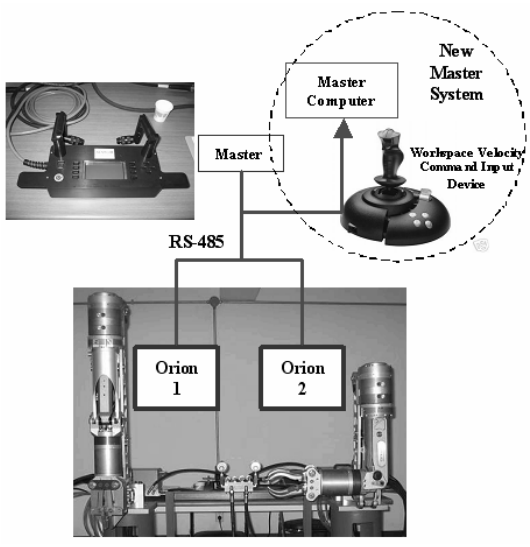

Fig. 9. ORION manipulator system with new master system.

we can realize the optimization process and task-oriented control. This kind of master system has a greater advantage for some tasks requiring accurate motion of end-effecter such as coring, drilling and underwater connector mating. The velocity reference commanded from the input device in the workspace is solved to joint reference in the master computer, and it is transferred to the slave manipulator through RS-485 serial communication. To reject the various uncertainties in a real situation, we synthesize feedback control for given manipulation variables as follows:

$$\dot{r}_1 = \dot{r}_1^d + G(r_1^d - r_1)\,, \tag{22}$$

where $\dot{r}_1^d$ is the desired velocity of the end-effecter given by workspace-command-input device, and G is the constant gain matrix that guarantees stability of the linear system. Substituting (22) to (21), we have reference velocity $\dot{q}_r$ in joint space by

$$\dot{q}_r = J_1^+\left(\dot{r}_1^d + G(r_1^d - r_1)\right) + \left\{E_n - J_1^+ J_1\right\}\left(-\varepsilon\frac{\partial p}{\partial q}\right)^T . \tag{23}$$

Then the position command of the slave manipulator is given by

$$q_r = q + \dot{q}_r \Delta t\,, \tag{24}$$

where q is current joint angle and Δt is sampling time. Eqs. (23) and (24) will be used in experiments with the ORION manipulator system.

5. Conclusion

This paper presents a task-oriented manipulability analysis of a tele-operated robotic arm for a remotely operated vehicle (ROV) and its application to task-oriented joint configuration. To reduce the tele-operator's burden in performing underwater tasks, a new master system is introduced so that the operator can command a slave manipulator in task space. The redundancy generated according to specific tasks is utilized to enhance the functionality of the manipulator. Task-oriented manipulability is defined as manipulability acquired from a task-oriented Jacobian matrix. The task-oriented Jacobian matrix is obtained by selecting the row vectors connected to a required task. The task-oriented manipulability measure is used to find the optimal posture in off-line and to control the tele-operated manipulator in on-line. The task-oriented manipulability analysis with an underwater manipulator, ORION manipulator, is carried out in a given posture. A scalar function composed of TOMM and JML is proposed. The optimal postures of the manipulator are found by SQP adopting the scalar function as an objective function and end-effecter position as an equality constraint. In order to utilize the redundancy in on-line control, we use redundancy resolution based on the pseudo inverse of the task-oriented Jacobian matrix adopting the scalar function as a performance index. A numerical simulation with the proposed method demonstrates that 1) the task-oriented manipulability analysis is able to give a measure of subtask ability of tele-operated manipulators (Fig. 3), 2) optimized posture in the sense of TOMM and JML can be obtained successfully (Fig. 4), 3) task-oriented control can achieve given tasks with higher TOMM and JML (Fig. 4 and Fig. 5). Experimental tests with the new master system will be performed in the near future.

Acknowledgment

This work was supported by the Ministry of Marine Affairs and Fisheries (MOMAF) of Korea for the development of a deep-sea unmanned underwater vehicle.

References

[1] G. Antonelli, F. Caccavale, S. Chiaverini and L. Villani, Tracking control for underwater vehicle-manipulator systems with velocity estimation, *IEEE J. of Oceanic Engineering,* 25 (3) (2000) 399-413.

[2] M. W. Dunnigan and G. T. Russell, Evaluation and reduction of the dynamic coupling between a manipulator and underwater vehicle, *IEEE J. of Oceanic Engineering,* 23 (3) (1998) 260-273.

[3] N. Sarkar and T. K. Podder, Coordinated motion planning and control of autonomous underwater vehicle-manipulator systems subject to drag optimization, *IEEE J. of Oceanic Engineering,* 26 (2) (2001) 228-239.

[4] S. S. You, Diving Autopilot Design for Underwater Vehicle Using Multi-Objective Control Synthesis, *KSME International J.,* 12 (6) (1998) 1116-1125.

[5] Y. Nakamura, Advanced robotics redundancy and optimization, Addison-Wesley Publishing company, (1991).

[6] S. Chiaverini, Singularity-robust task-priority redundancy resolution for real-time kinematic control of robot manipulators, *IEEE Transactions on Robotics and Automation,* 13 (3) (1997) 398-410.

[7] T. Yoshikawa, Manipulability of robot mechanisms, *International J. of Robotics Research,* 4 (2) (1985) 3-9.

[8] T. Yoshikawa, Dynamic manipulability of robot manipulators, *J. of Robotics Systems,* 2 (1) (1985) 113-124.

[9] S. Lee, Dual redundant arm configuration optimization with task-oriented dual arm manipulability, *IEEE Transactions on Robotics and Automation,* 25 (1) (1999) 78-97.

[10] J. Lee, Velocity workspace analysis for multiple arm robot systems, *Robotica,* 19 (2001) 581-591.

[11] P. Chiacchio, Y. Bouffard-Vercelli and F. Pierrot, Force polytope and force ellipsoid, *J. of Robot System,* 14 (8) (1997) 613-620.

[12] Dual orion 7P & 7PE manipulator systems technical mannual, ALSTOM Schilling Robotics (2002).